

SIMPLE EXPLICIT MODEL OF LIQUID MEAN FLOW IN REGION ABOVE AXIAL IMPELLER*

Miloslav HOŠŤÁLEK^a and Ivan FOŘT^b

^a *Institute of Inorganic Chemistry, 400 60 Ústí nad Labem and*

^b *Prague Institute of Chemical Technology, 166 28 Prague 6*

Received December 21st, 1983

The study describes a method of modelling axial-radial circulation in a tank with an axial impeller and radial baffles. The proposed model is based on the analytical solution of the equation for vortex transport in the mean flow of turbulent liquid. The obtained vortex flow model is tested by the results of experiments carried out in a tank of diameter 1 m and with the bottom in the shape of truncated cone as well as by the data published for the vessel of diameter 0.29 m with flat bottom. Though the model equations are expressed in a simple form, good qualitative and even quantitative agreement of the model with reality is stated. Apart from its simplicity, the model has other advantages: minimum number of experimental data necessary for the completion of boundary conditions and integral nature of these data.

Among the great number of diverse approaches to the modelling of charge flow in mechanically agitated equipments the simplest quantitative models postulate potential liquid flow. A correspondent notion for the case of stirred charge is the concept of Rankin (potential) vortex¹, used for the representation of tangential flow regime in an unbaffled tank. Further potential flow models for axial-radial liquid flow (in baffled vessels) have been published, *e.g.* by De Souza and Pike², Fořt and coworkers³, and others^{4,5}. In spite of considerable idealization of circumstances in described system the models are favourable for their simplicity and descriptiveness. A more realistic approach to the modelling of real liquid flow, however, respects its vorticity. An explicit model of vortex flow for a tank without baffles has been published, *e.g.* by Martynov⁶, another one for baffled tank, *e.g.* by Hošťálek and Fořt⁷. Among models based on the numerical solution of motion equation, *e.g.*^{8,9} may be mentioned. Although the possibilities of contemporary computer technique are undoubtedly great and the numerical algorithm sufficiently effective, such extensive calculations as in the above approaches may not — due to various causes — be possible to realize or even in all cases necessary. Our study shall be focused on the derivation and verification of the simple explicit model of the vortex flow of liquid, facilitating the presentation of the experimental data of flow in the major part of liquid volume above the level of axial impeller.

* Part LXIII in the series Studies on Mixing; Part LXII: This Journal 50, 930 (1985).

THEORETICAL

Let us consider the agitated system represented in Fig. 1. A vertical cylindrical tank with profiled (or even flat) bottom is filled with homogeneous newtonian liquid. Its turbulent flow regime is maintained by means of an axial high-speed impeller. The impeller is placed in the vessel axis, rotates with a constant frequency, creating a flow of liquid towards the vessel bottom. The tangential flow is suppressed by vertical baffles placed at regular intervals along the vessel wall and reaching from the liquid surface to the bottom. The origin of a system of cylinder coordinates (r, φ, z) shall be placed in the plane of the lower edge of the cylindrical part of the vessel.

For statistically averaged flow field (so-called mean flow) the momentum transport is described by the Reynolds equation. In contrast to the laminar flow equation it is characterized – apart from the viscous (Newton) shear stress – by an additional (Reynolds) stress caused by turbulence¹⁰. Using Bussinesque's approach, also this stress may be considered proportional to the mean velocity gradient with a proportion coefficient called dynamic eddy (vortex) viscosity μ_t . Under ordinary turbulent flow regime the value of this coefficient is some orders higher than in case of Newton, *i.e.* $\mu_t \gg \mu$. The influence of the so-called diffusion members of motion equations may be considered – in case of turbulent flow – much more significant than it would result from the similarity theory applied to the equations of laminar flow.

Let us now assume that μ_t is a constant scalar (a usual conception). In the case of a quasistationary two-dimensional flow, when we neglect the influence of inertial forces on the viscous and especially turbulent friction forces, we may obtain an equation corresponding in its form to the Stokes simplification of motion equations¹¹

$$E^2(E^2\bar{\psi}) = 0, \quad (1)$$

where $\bar{\psi}$ is the Stokes stream function for the mean flow by

$$\bar{w}_r = \frac{\partial \bar{\psi}}{r \partial z}, \quad \bar{w}_z = -\frac{\partial \bar{\psi}}{r \partial r} \quad (2a, 2b)$$

and E^2 represents differential operator

$$E^2 = \frac{\partial^2}{\partial r^2} - \frac{\partial}{r \partial r} + \frac{\partial^2}{\partial z^2}. \quad (3)$$

Eq. (1) is a linear partial differential equation of the fourth order. The boundary conditions of its solution are introduced in Fig. 2. The aim of modelling is to obtain a description of liquid flow in the stirred tank, within the space limited by the planes $z = z_0 (\cong H_2 + h_m)$ and $z = H$ (liquid surface). The liquid flow in the mixing

tank enters this space through the annulus $(r_2, D/2)$ in the horizontal plane z_0 and leaves it after circulation in the circle with diameter r_2 lying in the same plane z_0 . The overall flowrate of liquid through the investigated space is characterized by the stream function value $\bar{\psi}_C = \bar{\psi}_C(r_2, z_0)$. It consists both of the so-called primary flow passing also through the impeller rotor region and of a certain flow fraction due to the momentum exchange with the primary flow (secondary or induced flow). The boundary between the primary and induced flows is characterized by the value of stream function $\bar{\psi}_P$. To facilitate the application of boundary conditions in the solution of (1), the investigated space may be divided into cylindrical region A and regions B and C of the shape of hollow cylinder; the radii of the boundary cylindrical surfaces $r = r_1$ and $r = r_3$ being chosen so that region A and C might be passed by the primary flow only.

In thus divided tank volume the fulfilment of the following boundary conditions shall be required:

vessel axis/wall

$$\bar{\psi} = 0, \quad \partial \bar{w}_z / \partial r = 0, \quad r = \begin{cases} 0 \\ D/2 \end{cases}, \quad z \in \langle z_0, H \rangle; \quad (4)$$

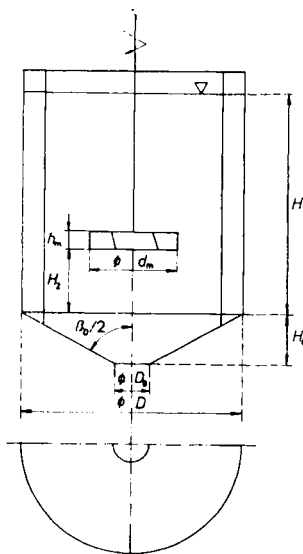


FIG. 1
Sketch of mixing system

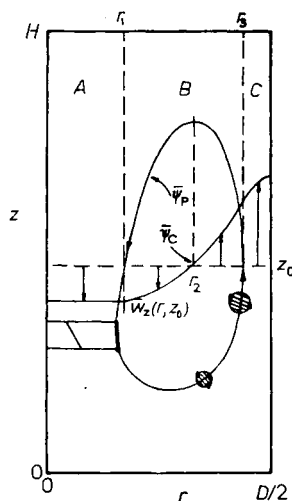


FIG. 2
Delineation of investigated volume and of its further division

boundary of regions A and B

$$\bar{w}_r = -\bar{\psi}_p/r_1(H - z_0), \quad \partial\bar{w}_z/\partial r = 0, \quad r = r_1, \quad z \in \langle z_0, H \rangle; \quad (5)$$

boundary of regions B and C

$$\bar{w}_r = -\bar{\psi}_p/r_3(H - z_0), \quad \partial\bar{w}_z/\partial r \geq 0, \quad r = r_3, \quad z \in \langle z_0, H \rangle; \quad (6)$$

plane of upper bases of regions A, B, C (liquid surface)

$$\bar{\psi} = 0, \quad r \in \left\langle 0, \frac{D}{2} \right\rangle, \quad z = H; \quad (7)$$

plane of lower bases of regions A, B, C

$$\bar{w}_z = -2 \frac{\bar{\psi}_p}{r_1^2}, \quad r \in \langle 0, r_1 \rangle, \quad z = z_0; \quad (8a)$$

$$\frac{\partial\bar{w}_z}{\partial r} \geq 0, \quad \frac{\partial^2\bar{w}_z}{\partial r^2} > 0, \quad r \in \langle r_1, r_3 \rangle, \quad z = z_0; \quad (8b)$$

$$\frac{\partial\bar{w}_z}{\partial r} = \Omega, \quad r = r_3, \quad z = z_0; \quad (8c)$$

$$\frac{\partial\bar{w}_z}{\partial r} \geq 0, \quad \frac{\partial^2\bar{w}_z}{\partial r^2} < 0, \quad r \in \left\langle r_3, \frac{D}{2} \right\rangle, \quad z = z_0. \quad (8d)$$

Boundary conditions (4) to (6) indicate a linear dependence of function $\bar{\psi}$ on the axial coordinate as possible solution of (1) for all the three regions. Using the methods of separation of variables and variation of constants¹¹ the solution of (1) may be obtained as

$$\bar{\psi} = (a + br^2 + cr^2 \ln r + dr^4)(1 + ez). \quad (9)$$

With regard to definition relations (2) equations for mean velocity components may also be expressed

$$\bar{w}_r = (a/r + br + cr \ln r + dr^3) e, \quad (10)$$

$$\bar{w}_z = -(2b + c + 2c \ln r + 4dr^2)(1 + ez). \quad (11)$$

In relations (9) to (11) five integration constants a, b, c, d , and e occur, which must be determined from the boundary conditions of A, B, C .

The boundary condition for liquid surface (7) implies that the parameter e must in all regions fulfil

$$e(X) = -1/H, \quad X = A, B, C. \quad (12)$$

The determination of the remaining four parameters requires the solution of a system of four linear equations for each of the regions. For instance for A we may thus obtain

$$a(A) = 0, \quad b(A) = \frac{1}{r_1^2} \frac{H}{H - z_0} \bar{\psi}_P, \quad c(A) = 0, \quad d(A) = 0. \quad (13)$$

The relations for the calculation of these parameters in regions B and C are summed up in Table I. Given the values of $\bar{\psi}_P$ and Ω , the so far introduced relations enable us to calculate the field of stream function $\bar{\psi}$ values and/or of velocity components \bar{w}_r and \bar{w}_z in any of the regions A, B , and C if the positions of the interfacing planes $r = r_1$ and $r = r_3$ are also given. Because, according to the real situation, the solution should be continuous even on these boundaries, the introduced quantities must be specified by further conditions

$$\bar{w}_z|_{r \rightarrow r_1^-} = \bar{w}_z|_{r \rightarrow r_1^+}, \quad \bar{w}_z|_{r \rightarrow r_3^-} = \bar{w}_z|_{r \rightarrow r_3^+}. \quad (14a, 14b)$$

By numerical solution of the last non-linear system of continuity conditions we may calculate the coordinates of cylindrical surfaces r_1 and r_3 corresponding to the given values $\bar{\psi}_P$ and Ω . In case the boundary conditions of the solution are given by the two values of stream function $\bar{\psi}_P$ and $\bar{\psi}_C$ further conditions

$$\bar{w}_z(r_2, z) = 0, \quad \bar{\psi}(r_2, z_0) = \bar{\psi}_C \quad (15a, 15b)$$

must be fulfilled. From conditions (14) and (15) we may calculate for these specific values $\bar{\psi}_P$ and $\bar{\psi}_C$ the values of parameters r_1, r_2, r_3 , and Ω .

EXPERIMENTAL

The verification of the model is based on our published results⁷ measured in the tank with conical bottom (further called system 1) and on the data¹² for (standard) configuration with a flat bottom (system 2). The basic features of both systems are apparent from Fig. 1. The impeller used had in all cases six blades with an inclination angle 45° and was in accordance with the respective standard¹³. There were four radial baffles in the vessel, their width being equal to a tenth of vessel diameter D . The cylindrical part of the vessel was filled with water up to the height H equal to D .

The measurements of velocity profiles took always place in an axial-radial plane lying in the middle between two neighbouring baffles. Some further geometrical and other parameters were specific for the given systems:

System 1 (tank of diameter 1 m with conical bottom): The vertex angle of the bottom was $\beta = 120^\circ$ and the diameter of its smaller base D_0 (Fig. 1) amounted to one sixth of D . On the whole, two configurations have been investigated: one with an impeller of diameter $d_m = 0.333$ m and rotational frequency $n = 180 \text{ min}^{-1}$, the other characterized by $d_m = 0.400$ m and rotational frequency $n = 125 \text{ min}^{-1}$. The plane of lower edges of impeller blades was always coincident

TABLE I
Relations for calculation of model parameters in regions B and C

Parameter (region)	Calculation formula
$a(B)$	$\left[\bar{\psi}_P - \frac{r_3^3 r_1^2 (r_3^2 - r_1^2) - 4r_1^4 \ln(r_3/r_1)}{8 (r_3^2 - r_1^2)^2} \Omega \right] \frac{H}{H - z_0}$
$b(B)$	$\frac{r_3 r_3^4 - r_1^4 - 4r_1^2 (r_3^2 \ln r_3 - r_1^2 \ln r_1)}{8 (r_3^2 - r_1^2)^2} \Omega \frac{H}{H - z_0}$
$c(B)$	$\frac{r_3}{2} \frac{r_1^2}{r_3^2 - r_1^2} \Omega \frac{H}{H - z_0}$
$d(B)$	$-\frac{r_3}{8} \frac{1}{r_3^2 - r_1^2} \Omega \frac{H}{H - z_0}$
$a(C)$	$\left\{ \frac{\bar{\psi}_P}{(D/2)^2 - r_3^2} + \frac{1}{2} \left[\frac{r_3^3 \ln r_3}{(D/2)^2 - r_3^2} + \frac{r_3^3}{4} \frac{1 - 4 \ln(D/2) - (2/D)^2 r_3^2 (1 - 4 \ln r_3)}{(D^2/4 - r_3^2)^2} \frac{D^2}{4} \right] \Omega \right\} \frac{D^2}{4} \frac{H}{H - z_0}$
$b(C)$	$-\left\{ \frac{\bar{\psi}_P}{(D/2)^2 - r_3^2} + \frac{1}{2} \left[\frac{r_3^3 \ln r_3}{(D/2)^2 - r_3^2} + \frac{r_3 (D/2)^4}{4} \frac{1 - 4 \ln(D/2) - (2/D)^4 r_3^4 (1 - 4 \ln r_3)}{(D^2/4 - r_3^2)^2} \right] \Omega \right\} \frac{H}{H - z_0}$
$c(C)$	$-\frac{r_3}{2} \frac{(D/2)^2}{(D/2)^2 - r_3^2} \Omega \frac{H}{H - z_0}$
$d(C)$	$\frac{r_3}{8} \frac{1}{(D/2)^2 - r_3^2} \Omega \frac{H}{H - z_0}$

with that of the lower base of the cylindrical part of the tank (height $H_2 = 0$). For the determination of the direction and value of the mean velocity a five-hole Pitot tube was used¹⁴. The measurements yielded a progression of radial profiles of the components \bar{w}_r , \bar{w}_ϕ , and \bar{w}_z for the values of axial coordinate z : (0–0.167–0.333) and 0.500 m.

System 2 (flat-bottomed tank of diameter 0.29 m): The results of measurements by means of a three-hole Pitot tube in a flat-bottomed vessel (Fig. 1 – $\beta_0 = 180^\circ$ and $H_0 = 0$) have been published by Fořt, Neugebauer, and Pastyříková¹². The investigated configurations include impellers of three different sizes (the diameter d_m was 58, 73, and 97 mm) at three rotational frequencies (ranging from 360 min^{-1} for the largest impeller to 1300 min^{-1} for the smallest one). The height of the impeller above the vessel bottom was in all cases $H_2 = 73 \text{ mm}$.

The measurements yielded the radial profile of \bar{w}_z in the distance of 10 mm from the plane of the upper edges of impeller blades. The individual sections of this profile were always represented by regression lines.

The survey of main geometrical parameters of both systems is given in Table II.

TABLE II
Survey of main geometrical parameters of individual configurations

System	D , mm	H_2 , mm	β_0 , deg.	D_0 , mm	d_m , mm	h_m , mm
1	1 000	0	120	150	333	67
1	1 000	0	120	150	400	80
2	290	73	180	150	58	12
2	290	73	180	150	73	15
2	290	73	180	150	97	19

TABLE III
Survey of flow model parameters

Parameter	System 1		System 2			
	Original	Calculated	$d_m/D = 0.333$	$d_m/D = 0.400$	$d_m/D = 0.200$	$d_m/D = 0.333$
H/D	—	1	1	1	1	1
z_0/D	—	0.333	0.333	0.317	0.317	0.382
Ψ_P/nd_m^3	—	0.145 ^a	0.115 ^a	0.119	0.119	0.160
Ψ_C/nd_m^3	—	0.200	0.170	0.170	0.507	0.312
—	r_1/D	0.316	0.297	0.140	0.140	0.237
—	r_3/D	0.454	0.456	0.485	0.485	0.466
—	Ω/n	3.99	5.24	1.16	1.16	4.25

^a Estimation.

RESULTS

To facilitate mutual comparison the results shall be given in dimensionless form. The length coordinates (and – analogously – the dimensions of equipment) are normalized by the tank diameter

$$r/D, \quad z/D. \quad (16)$$

Mean velocity components are given as the ratio to the velocity of impeller blade tips

$$\bar{w}_r/nd_m, \quad \bar{w}_z/nd_m \quad (17)$$

(leaving out the coefficient π). The stream function $\bar{\psi}$ will then be related to the value of the product of rotational frequency and of the cube of impeller diameter; the slope of the velocity profile Ω to the impeller rotational speed, *i.e.*

$$\bar{\psi}/nd_m^3, \quad \Omega/n. \quad (18)$$

The parameters of vortex flow model for the configurations of the mixing equipment denoted system 1 and system 2 are summed up in Table III (for the basic parameters see Table II). The remaining data in Table III represent the additionally calculated parameters: the delimitation of boundaries between regions A, B, and C (radii r_1 and r_3) as well as the value of the slope Ω . By substituting of the last mentioned values into relation (13) or into those in Table I we may obtain the numerical values of integration constants a , b , c , d , and e in regions A, B, and C. The results of modelling of the axial component of mean velocity \bar{w}_z for the level z_0 are given in Figs 3 and 4: for system 1 they are directly compared with measurement results, whereas for system 2, the theoretical curve is compared with the regression lines (dot-and-dash), by which the individual sections of measured profiles have been approximated¹². For system 1 Fig. 5 compares the model course of stream function in two axial planes with functions obtained directly from the experiments. And finally Fig. 6 shows the calculated streamlines field for system 1 (smaller impeller).

DISCUSSION

The real nature of the flow in the mixing tank is very complex. The extent of simplifications adopted in the process of modelling does not – on the whole – differ from the state in current practice. Here we have in mind especially the assumption of the suppression of the tangential component of motion in favour of that in the axial-radial plane by means of radial baffles, and the assumption of the axisymmetrical flow. The fulfilment of the assumption of the quasistationary nature of the process

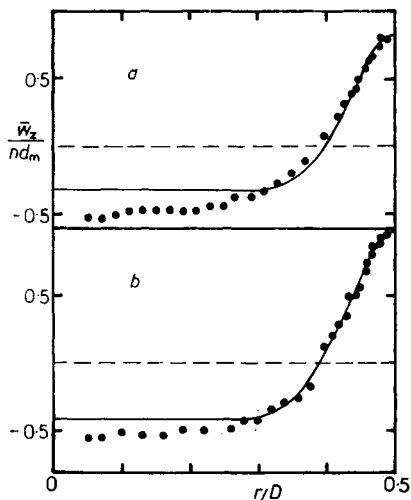


FIG. 3

Comparison of results of modelling \bar{w}_z (solid line) with experiments for lower base of investigated volume in system 1. *a* $d_m/D = 0.333$, $z_0/D = 0.33$; *b* $d_m/D = 0.400$, $z_0/D = 0.333$

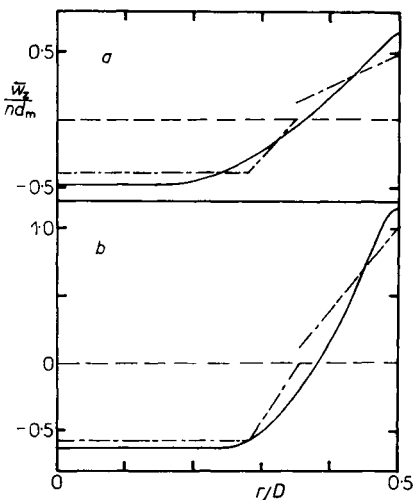


FIG. 4

Comparison of results of modelling \bar{w}_z (solid line) with experiments for lower base of investigated volume in system 2. *a* $d_m/D = 0.200$, $z_0/D = 0.317$; *b* $d_m/D = 0.333$, $z_0/D = 0.332$

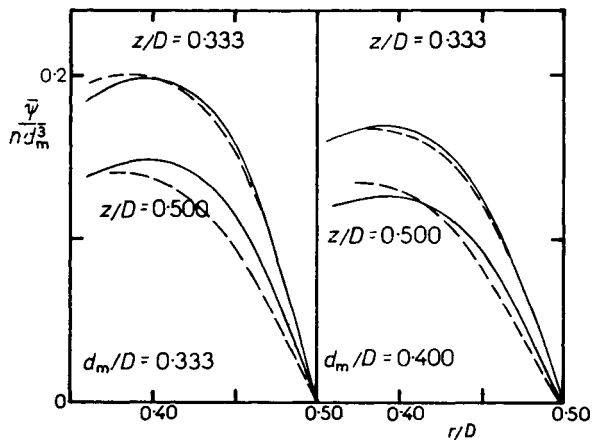


FIG. 5

Comparison of radial profiles of stream function $\bar{\psi}$ in flow close to wall according to given model (solid line) to course determined from measurement results (dashed line) for system 1

may as well be considered an acceptable approximation of the real state of liquid (a random motion caused by turbulence and a periodical motion produced by the impeller blades are superimposed to the mean flow of liquid). The above limitations have radically simplified the mathematical description but at the same time they implicitly determine the extent of accuracy which may be expected from the model. Our next step has been to attribute the principal part of vorticity transfer to bigger aggregates of charge – vortices – neglecting at the same time the influence of inertial and eventually even molecular forces. Kotchin and coworkers¹⁵ have stated for instance that in modelling turbulent liquid flow the viscosity coefficient in diffuse members of motion equations must be considered even six orders higher than the value corresponding to the laminar flow. The accepted flow model (1) could then be solved much more generally in accordance with the method⁷; here, however, we have concentrated on finding the solution in the closed form of a simple mathematical function. The simplicity of solutions (9), (10), and (11) which makes the model descriptive and easily applicable, was the result of the choice of boundary conditions. Homogeneous boundary conditions (4) and (7) for the stream function on the boundaries of the agitated system (*i.e.* in the vessel axis, on its wall and on the liquid surface) are in keeping with the physical meaning of its function as the extent of the volumetric flow rate of liquid (a closed system with respect to the stirred liquid).

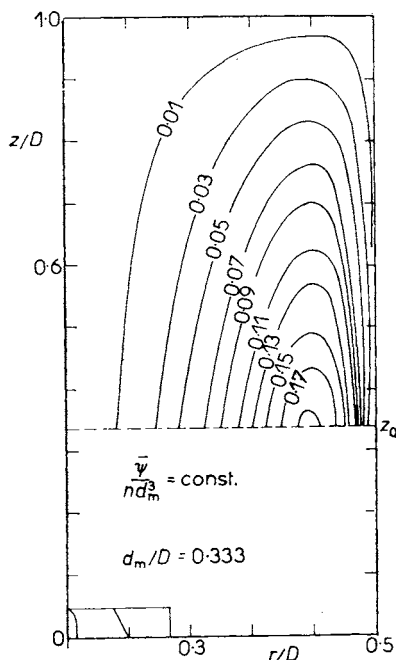


FIG. 6
Streamline field according to given model
in system I

The choice of mean velocity gradient in the above loci is rather more ambiguous. This holds mainly for the vessel wall (in the vessel axis we do not consider the influence of the impeller shaft due to its relatively small diameter). Here in reality the component of mean velocity gradient in the normal direction will have non-zero value and opposite sign than further in the charge flow, because of the influence of the solid wall to which the liquid sticks due to its viscosity (the maximum in the radial profile close to the wall, but not directly on it, has been mentioned *e.g.* by¹⁶). Hence, posing homogeneous boundary condition (4) we neglect the dimensions of the boundary layer, shifting the maximum of radial profile of \bar{w}_z as far as the vessel wall. As the piston nature of the axial profile of \bar{w}_r has been postulated (see conditions (5) and (6), or solution (10)), the negative slope of the radial profile of \bar{w}_z indicates also the value of the non-zero component of mean velocity rotation. The maximum value of this gradient is, according to conditions (8), postulated in the point (r_3, z_0) . This corresponds to the fact described *e.g.* by¹⁷ that just on the interface of the prominent primary flow leaving the impeller and the neighbouring liquid powerful vortices appear, which are afterwards carried off by the flow and finally vanish by diffusion into the environment (Fig. 2). According to the model, the primary flow with a homogeneous (piston) profile emerges from the considered space (see condition (8a) which is in keeping with the experimental data of reality).

The plane of lower bases of regions A, B, and C has been specified only very vaguely. A qualitatively correct flow description by means of the proposed model may be attained in case the plane z_0 is situated on the level of the centre of axial-radial circulation, *i.e.* in the point where the change of sign both in the radial profile of \bar{w}_r and in the axial profile of \bar{w}_z occurs (or above it). In such case the field of values \bar{w}_r would have the same sign in the whole investigated space, which is just what the given model requires. The plane z_0 should not be chosen above the level where the fraction of secondary flow may extent. Otherwise, some of the premises of the model ought to be modified (*i.e.* the division into regions and some boundary conditions). For the specific case of system 1 the plane $z_0 = 0.333$ fulfilled the requirements most closely. In the nearest profile measured ($z = 0.500$ m) the model values of $\bar{\psi}$ are – in keeping with the reality – proportionally lower (Fig. 5). In system 2 we had to be satisfied with a single measured profile (respective z_0 see Table III). The quantities $\bar{\psi}_p$ and $\bar{\psi}_c$ are the only ones to be determined from the boundary conditions. These have been currently measured, especially $\bar{\psi}_p$. They are often assessed by means of a simple indicating particle method^{18,19}. When needed, the way of setting boundary conditions may be variously modified. *E.g.* for system 1 various $\bar{\psi}_p$ values were tried, until the model was in keeping with the measured section of the velocity profile at the vessel wall. For the repeated employment of the model, the fairly difficult calculation of radii r_1 , r_2 , and r_3 and the slope Ω may be carried out in advance for different values of the ratio $\bar{\psi}_p/\bar{\psi}_c$. The results in Fig. 7 show that with the increasing value of this simplex the radii r_1 , r_2 , and r_3 mutually approach, *i.e.* the

volume of region B diminishes. Fig. 8 illustrates the relation among individual boundary conditions. Here we can see that with increasing ratio of the primary flow the absolute value of Ω increases. This value is at the same time directly proportional to the total liquid flowrate and indirectly proportional to the cube of tank diameter D^3 . (Note: At given values of r_1 and r_3 the quantity Ω may be expressed explicitly from condition (14b).)

Now we shall compare the results of model application with reality. The direct comparison can be made in Fig. 3. It implies that in system 1 there is almost a perfect agreement in the ascending flow region close to the wall (but cp. the discussion of the calculation method). In the flow close to the vessel axis descending back to the impeller, the experimentally found flow rate values are higher than the model ones. This may be explained either by an error in the measurement method or by a possible flow asymmetry caused by the baffles. From the results in Fig. 4 for system 2 it is however apparent that in this case the qualitative representation of "reality" by means of the model is much less accurate, especially in the flow close to the wall: here the model assumes steeper radial profile of \bar{w}_z , especially for the smallest impeller used. This can — of course — be partly explained by the measurement error or by an error in statistic interpretation of the measured profile sections, but there may even be some deeper cause, for instance lower turbulence intensity in the smaller of the two mixing equipments (see the model assumption of neglecting the influence of inertial

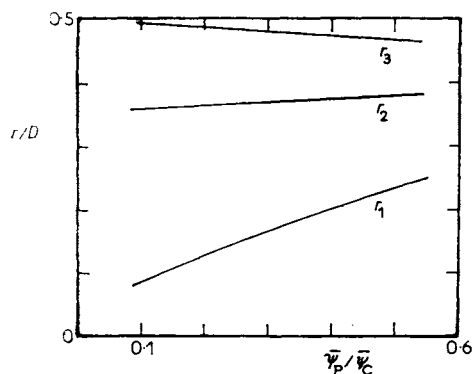


FIG. 7

Radius of cylindrical surface separating regions A and B ($r = r_1$) or B and C ($r = r_3$) and radial coordinates of change of flow direction from ascending to descending in region B ($r = r_2$) in dependence on ratio $\bar{\psi}_p/\bar{\psi}_c$ for given model

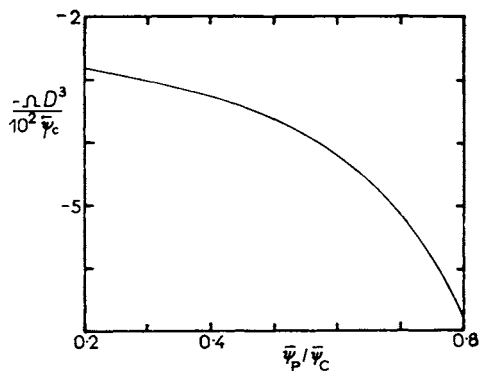


FIG. 8

Illustration of relations among model boundary conditions for different variants of introduced data

forces). In spite of these facts, the agreement between the data predicted and found may be considered sufficient.

Thus we have verified the properties of the model in the description of radial profiles of \bar{w}_z and $\bar{\psi}$. For axial profiles of these quantities the model prescribes a simple linear dependence. In this case, there is a much smaller number of experimental data for a quantitative assessment. Starting from Fig. 5, however, we may – even from this viewpoint – observe at least a qualitative agreement from the case of the stream function: *e.g.* in the profile corresponding to 1/4 of the model space height ($z/D = 0.500$) the model for the alternative of the smaller impeller predicted values 13% higher than these assessed from the experiments in the first type of mixing equipment; the error in the case of smaller impeller was considerably smaller. The distribution of streamline field in Fig. 6 implies that the model description of the investigated volume is in keeping with current physical ideas: the continuity of streamlines and their smooth transition across the region interfaces.

CONCLUSION

The study solved a simplified transport equation of vorticity for a baffled system with an axial high-speed impeller. From the obtained relations the fields of radial and axial mean velocity components and the stream functions in the major part of the volume between the impeller and the liquid surface may be calculated. Model ideas have been tested by means of our own experiments or by the published data for different tank and impeller sizes (diameters 1 m and 0.29 m and the value of simplex d_m/D ranging from 0.200 to 0.400, respectively), different shape of tank bottom (flat or conical) and the impeller rotational frequency ranging from 125 min^{-1} to 1 300 min^{-1} . A good agreement of the tested model with reality has been stated. For the numerical solution of the model relation only the primary flow rate and the total volumetric flow rate in the chosen region must be given. The main advantage of the proposed model is the simplicity of the relations obtained and their explicit character, which makes it descriptive and easily applicable. The model may be used either directly or with simple modifications according to the structure of the available experimental data. After some arrangements (using the auxiliary diagrams in repeated calculations) the computation may be carried out by means of an efficient pocket calculator.

LIST OF SYMBOLS

- A region according to Fig. 2
- a integration constant ($\text{m}^3 \text{s}^{-1}$)
- B regions according to Fig. 2
- b integration constant (m s^{-1})
- C region according to Fig. 2

c	integration constant (m s^{-1})
D	mixing tank diameter (m)
D_0	diameter of lower base of tank bottom in shape of truncated cone (m)
d	integration constant ($\text{m}^{-1} \text{s}^{-1}$)
d_m	impeller diameter (m)
E^2	differential operator defined by Eq. (3)
e	integration constant (m^{-1})
H	height of liquid in cylindrical part of tank (m)
H_0	height of conical bottom (m)
H_2	height of lower edges of impeller blades above lower edge of cylindrical part of tank (m)
h_m	impeller blade height (m)
n	impeller rotational frequency (s^{-1})
r	radial coordinate (m)
r_1	radius of cylindrical surface separating regions B and C (m)
r_2	radial coordinate of turn of flow from ascending to descending direction (m)
r_3	radius of cylindrical surface separating regions B and C (m)
\bar{w}	liquid mean velocity (m s^{-1})
X	auxiliary variable
z	axial coordinate (m)
z_0	plane of lower bases of regions A, B, C (m)
β_0	vertex angle of tank bottom (1)
μ	dynamic viscosity ($\text{kg m}^{-1} \text{s}^{-1}$)
φ	tangential coordinate (1)
$\bar{\psi}$	Stokes stream function ($\text{m}^3 \text{s}^{-1}$)
Ω	boundary condition defined by Eq. (8a) (s^{-1})

Subscripts

C	total flow rate through given cross-section
P	primary flow
r	radial component
z	axial component
φ	tangential component

REFERENCES

1. Strek F.: *Míchání a míchací zařízení*. Published by SNTL, Prague 1977.
2. De Souza A., Pike R. W.: *Can. J. Chem. Eng.* 50, 15 (1972).
3. Fořt I., Obeid A., Březina V.: *This Journal* 47, 226 (1982).
4. Fořt I., Jaroš O., Hošťálek M.: *This Journal* 42, 3555 (1977).
5. Fořt I., Gračková Z., Koza V.: *This Journal* 37, 2371 (1971).
6. Martynov Yu. V.: *Teor. Osn. Khim. Tekhnol.* 14, 575 (1980).
7. Hošťálek M., Fořt I.: *This Journal* 50, 930 (1985).
8. Dutta A., Ryan M. E.: *AIChE J.* 28, 220 (1982).
9. Bergmann L., Naue G., Wolf P.: *Wiss. Z. TH Leuna-Merseburg* 23, 282 (1982).
10. Bird R. B., Stewart W. E., Lightfoot E. N.: *Transport Phenomena*. Wiley, New York 1965.
11. Jenson V. G., Jeffreys G. V.: *Mathematical Methods in Chemical Engineering*. Academic Press, London 1963.

12. Fořt I., Neugebauer R., Pastyřiková M.: *This Journal* 36, 1769 (1971).
13. Standard No 6910. VÚCHZ Chepos, Brno 1969.
14. Krátký J., Fořt I., Kroužilová Z., Drbohlav J.: *Sb. Vys. Šk. Chemicko-Technol. Praze K5*, 33 (1971).
15. Kotchin N. E., Kibel' I. A., Roze N. V.: *Teoreticheskaya Gidromekhanika*. GIFML, Moscow 1963.
16. Fořt I., Placek J., Strek F., Jaworski Z., Karcz J.: *This Journal* 44, 684 (1979).
17. Tatterson G. B., Yuan H. H. S., Brodkey R. S.: *Chem. Eng. Sci.* 35, 1369 (1980).
18. Fořt I.: *This Journal* 32, 3663 (1967).
19. Fořt I., Kudrna V., Valešová H.: *This Journal* 36, 164 (1971).

Translated by M. Procházka.